

CrystEngComm

Accepted Manuscript



This is an *Accepted Manuscript*, which has been through the Royal Society of Chemistry peer review process and has been accepted for publication.

Accepted Manuscripts are published online shortly after acceptance, before technical editing, formatting and proof reading. Using this free service, authors can make their results available to the community, in citable form, before we publish the edited article. We will replace this *Accepted Manuscript* with the edited and formatted *Advance Article* as soon as it is available.

You can find more information about *Accepted Manuscripts* in the [Information for Authors](#).

Please note that technical editing may introduce minor changes to the text and/or graphics, which may alter content. The journal's standard [Terms & Conditions](#) and the [Ethical guidelines](#) still apply. In no event shall the Royal Society of Chemistry be held responsible for any errors or omissions in this *Accepted Manuscript* or any consequences arising from the use of any information it contains.

ARTICLE

Twinning boundary-elongated hierarchical Pt dendrites with an axially twinned nanorod core for excellent catalytic activity

Cite this: DOI: 10.1039/x0xx00000x

Received 00th xxxxxx 20xx,
Accepted 00th xxxxxx 20xx

DOI: 10.1039/x0xx00000x

www.rsc.org/

Nguyen Tien Khi,^a Jisun Yoon,^a Hionsuck Baik,^b Sangmin Lee,^c Dongjune Ahn,^d
Seong Jung Kwon,^{*c} Kwangyeol Lee^{*a}

Twinning boundary elongated hierarchical Pt nanostructures with an excellent electrocatalytic activity are prepared by using axially twinned Pt₃Ni nanorods as the platform for epitaxial transfer of a twinned crystal structure. The high electrocatalytic activity of the hierarchical nanostructures results from the synergistic effects of lattice mismatch between Pt₃Ni core and Pt shell as well as the elongated twinning boundary.

Introduction

The catalytic activity of a nanoparticle is greatly affected by the proportion of highly energetic structural features¹⁻⁸ in the entire nanostructure as well as by its surface area.⁹ Accordingly, the preparation of facet-controlled nanoparticles exposing high energy facets, steps, and kinks¹⁻⁸ and core-shell nanoparticles with lattice mismatch between core and shell has been extensively pursued to render high surface energy to a nanoparticle.¹⁰⁻¹³ Recently, we have found that the presence of twinning boundary on the nanoparticle surface greatly enhances the catalytic activity.^{14,15} The highly energetic nature of twinning boundary, however, usually leads to the formation of nanostructures with minimized exposure of twinning coastline, although extended coastline of twinning boundary might be greatly beneficial to the catalytic activity.^{14,16} On the other hand, the highly energetic twinning boundary of an axially twinned nanorod could serve as a preferred nucleation site for the growth of nanocrystals because the growth of new nanocrystals on it would provide the desired surface energy minimization to the original twinning boundary.¹⁷⁻¹⁹ The epitaxial growth of a nanocrystal on the twinning boundary would transfer the twinning property to the newly grown nanostructures, leading to the elongation of energetic twinning boundary on the surface of the resulting nanostructure. Furthermore, by growing new crystallites with a different composition on the existing twinning boundary, it would be feasible to create a highly energetic surface due to the presence of lattice mismatch between the original twinned nanostructure and newly grown nanocrystallites. Such a twinning boundary coastline-elongated nanostructure is expected to possess high catalytic activity due to i) high surface area, ii) highly active extended twinning boundary at the surface, and iii) surface energy elevating lattice mismatch between core and shell.

Herein, we report the proof-of-concept experiment for the formation of a twinning boundary maximized Pt₃Ni@Pt heterohierarchical nanostructure by growing Pt nanodendrites on axially twinned nanorods of Pt₃Ni as well as its excellent catalytic activities towards methanol oxidation reaction.

Results and discussion

The transmission electron microscopy (TEM) and high resolution TEM (HRTEM) images of hierarchical heteronanostructures are shown in Fig. 1. Thin Pt₃Ni nanorods with diameters of 2~3 nm were prepared by using a procedure modified from the synthetic condition for five-fold Pt nanorods (See ESI for synthetic details). The Pt₃Ni nanorods are axially twinned as clearly seen in Figure 1b. However, it is difficult to discern exact twinning nature such as five-fold twinning of related Pt nanorods due to the difficulty in vertical alignment of thin nanorods. The energy dispersive X-ray spectrum study demonstrates the elemental composition of 3/1 (Pt/Ni) for the Pt₃Ni nanorods (ESI Fig. S2). Small Pt nanocrystals could be grown on the twinning boundary of axially twinned Pt₃Ni nanorods (Fig. 1a, b) via ethylene glycol-assisted thermal decomposition of Pt(acac)₂ at low temperatures. In a typical synthesis, Pt₃Ni nanorod (~ 2 mg) were dispersed in a mixture of Pt(acac)₂ (0.05 mmol), ethylene glycol (1.86 mmol) and octadecylamine (15 mmol) in a two-neck round bottom flask (15 mL) with a magnetic stirring at 80 °C. After being evacuated for 10 min with stirring at 80 °C, the resulting solution was kept at the same temperature for 20 h under Ar to give a worm-like heteronanostructure as shown in Fig. 1c. The HRTEM analysis of newly grown Pt nanocrystallites in Fig. 1d reveals that the twinned nature of the Pt₃Ni nanorod core is unaffected by the synthetic process and that crystal growth

behaviour is epitaxially transferred from the Pt₃Ni nanorod to Pt.

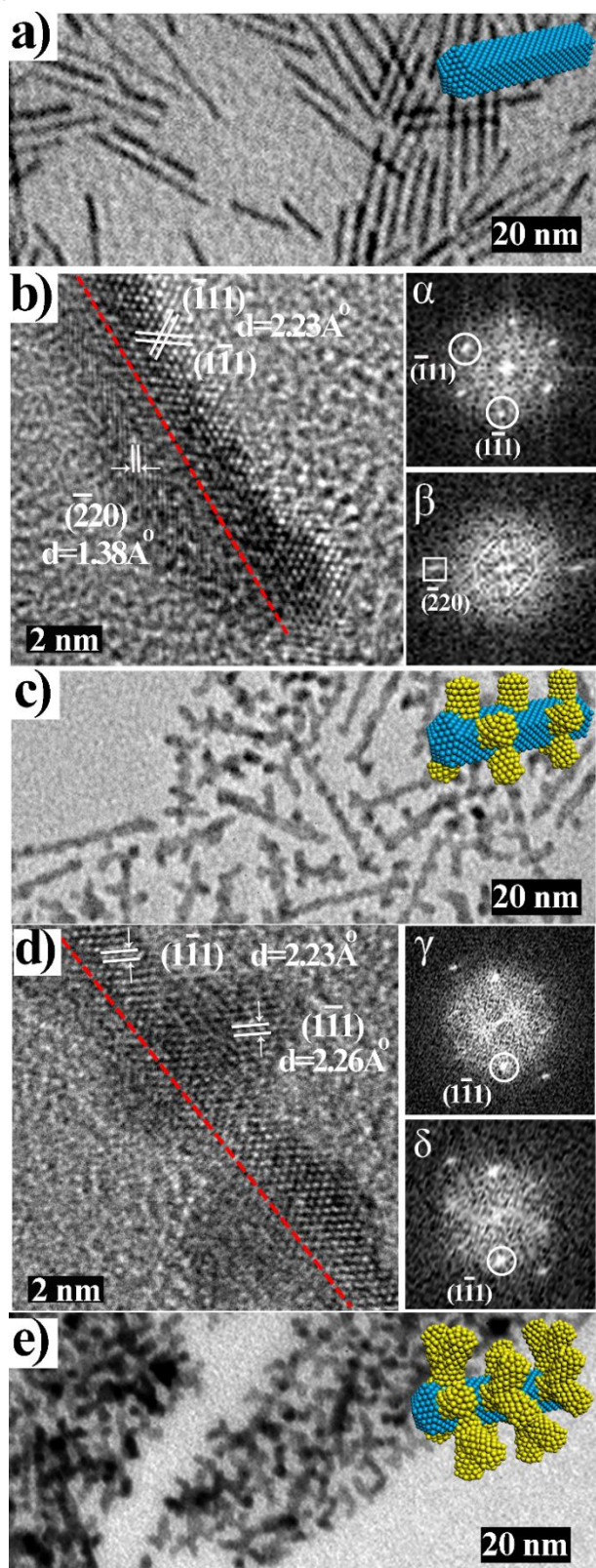


Fig. 1 TEM and HRTEM images of (a, b) thin Pt₃Ni nanorod (α , β : FFTs of right and left sides of Pt₃Ni nanorod) and (c, d) worm-like Pt₃Ni@Pt nanostructure (γ , δ : FFTs of branch and body parts in d). Red lines in b and d denote the twinning boundaries. (e) TEM image of dendritic Pt₃Ni@Pt.

The nanocrystallite formation on the side of a nanorod is completely different from the case of Rh nanoparticle growth at the tips of related Pt nanorods, which requires a higher decomposition temperature (> 130 °C) for the Rh(acac)₃ precursor and occurs only at the tips of nanorods.¹⁴ At high reaction temperatures, the binding of surface-stabilizing moieties on the nanorod tip might be selectively disturbed over the nanorod stem part to facilitate Rh nanocrystal growth.¹⁴ The lattice parameter discrepancies of 2.6% and 3.0% between Pt₃Ni and Pt and between Rh and Pt, respectively, are not very significant,²⁰ and therefore do not seem to be the main cause of the disparate regiospecific nanocrystal growth for different metals. At low reaction temperature of 80 °C of this study, there seems to be little reactivity difference between the {111} faceted nanorod tip and the {100} faceted middle part, as judged by indiscriminate formation of multiple nanocrystallites on the entire Pt₃Ni nanorod surface, which is counter-intuitive because the difference among different surface energies should be more pronounced at low temperatures. The absence of strongly protecting CO on the nanorod surface as well as the presence of multiple reactive twinning boundaries along the entire nanorod might have allowed the lateral growth of nanocrystallites on the Pt₃Ni nanorod; while CO as a reducing agent was crucial in the facilitated formation of Pt₃Ni nanorod at low temperatures, the growth of Pt phase on the surface of Pt₃Ni was not possible in the presence of CO, leading only to formation of non-attached Pt nanocubes. Close examination of HRTEM image in the Fig. 1d and the FFT images for the Pt₃Ni nanorod and for the newly grown Pt crystal reveals slight distortion in the crystal lattice at the boundary of Pt₃Ni phase and Pt phase due to the lattice mismatch, although the Pt nanocrystallites on the outermost roughened surface of the worm-like nanostructures seem to retain the atom packing behaviour of the Pt₃Ni core. The newly grown Pt nanocrystals do not exhibit preference for a specific facet stabilization in the absence of {100}Pt stabilizing CO.

The newly grown Pt crystallites on the surface of the worm-like nanostructures in Fig. 1c, d could serve as further nucleation and growth sites for Pt to eventually give dendritic nanostructures in Fig. 1e (See ESI for synthetic details). Interestingly, the diameter of the formed Pt nanocrystallites is kept under 2 nm, guaranteeing a very high surface area of the resultant hierarchical heteronanostructures. Hierarchical nanostructure of pure Pt with an identical structural motif could also be prepared similarly by using axially twinned Pt nanorods instead of Pt₃Ni nanorods (see ESI Fig. S1 for the structure and synthetic details).

There are little structural differences between hierarchical Pt@Pt nanostructure and hierarchical Pt₃Ni@Pt nanostructure. The only difference between the hierarchical structures of Pt@Pt and Pt₃Ni@Pt is the presence of the lattice mismatch between the core and shell; not much difference is expected for the twinning coastline proportion in the nanostructures. Therefore, if there is no catalytic contribution from the lattice mismatch between Pt₃Ni and Pt layers, there would be no activity difference between the hierarchical Pt@Pt

nanostructure and the hierarchical Pt₃Ni@Pt nanostructure. To investigate the influence of atomic distribution, namely, core-shell structure, and crystal twinning of the hierarchical nanostructure on the catalytic activity, the electrocatalytic properties toward methanol oxidation reaction (MOR) were examined for various Pt nanostructures, namely, axially twinned Pt nanorod, axially twinned Pt₃Ni nanorod, hierarchical Pt@Pt nanostructure, and hierarchical Pt₃Ni@Pt nanostructure. The Pt nanostructures-modified glassy carbon electrodes (GCEs) were electrochemically cleaned by scanning the potential between 0.0 V (vs. NHE) and 1.6 V several times in the electrolyte solution (0.5 M H₂SO₄) before obtaining cyclic voltammograms (CVs) in Fig. 2. The current densities, the mass activities, and the electrochemically active surface areas (ECSA) for the various nanostructures, which were determined by the hydrogen desorption method (See ESI), are shown in Table. 1.

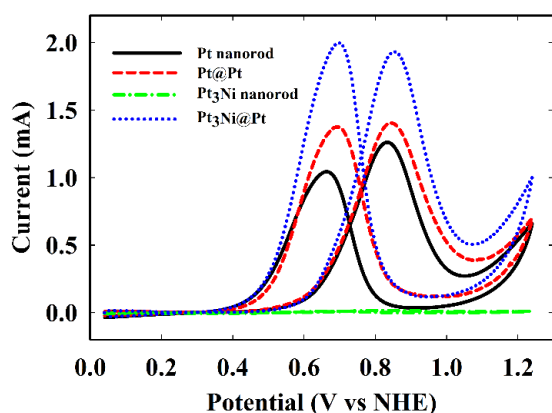


Fig. 2 Cyclic voltammograms of Pt nanostructures-modified GCE in 0.5 M MeOH + 0.5 M H₂SO₄ electrolyte solution. Scan rate was 50 mV/s.

Nanostructure	ECSA (m ² /g)	Current density (mA/cm ²)	Mass activity (mA/mg)
Pt nanorod	54.7	1.05	573
Pt@Pt	57.1	1.12	639
Pt ₃ Ni nanorod	1.6	0.46	7.5
Pt ₃ Ni@Pt	78.3	1.12	878

Table. 1 Electrocatalytic properties of various Pt nanostructures of this study for MOR

The cyclic voltammograms for the Pt nanostructure-modified GCE exhibited methanol oxidation peaks at ~0.8 V and ~0.6 V in the forward and the backward sweeps, respectively, which are consistent with typical methanol oxidation reaction patterns on Pt surface.²¹ The forward peak has been assigned to the methanol oxidation, while the backward peak stems from the oxidation of adsorbed CO or CO-like species generated via incomplete methanol oxidation. The methanol oxidation catalysed by Pt@Pt and Pt₃Ni@Pt seems to progress completely as judged by the nearly identical size of forward and backward peaks. The hierarchically dendritic Pt@Pt and Pt₃Ni@Pt nanostructures show enhanced mass activities over the Pt nanorods, which in turn exhibit much higher activity over {100}Pt nanocubes.²² Interestingly, Pt₃Ni nanorods showed very little catalytic activity toward MOR. While the low

catalytic activity of {100}Pt₃Ni for ORR has been previously explained, it is interesting to observe a similar low reactivity for MOR also.^{23,24} Specifically, Pt@Pt and Pt₃Ni@Pt dendritic hierarchical nanostructures show 10 % and 50 % increases, respectively, from that of Pt nanorods, likely due to the elongation of twinning coastline. The transfer of the twinning boundaries in the dendritic structures of this study has been greatly beneficial to the preservation of catalytic activity, while our previous attempt to form hierarchical nanostructure of Rh resulted only in the passivation of active sites, namely corners and edges.²⁵ Furthermore, the Pt₃Ni@Pt nanostructure shows the best performance, obviously due to the added contribution from lattice mismatch between the virtually catalytically inactive Pt₃Ni nanorod and newly grown Pt crystallites. This result implies that the usage of cheap core nanostructure with surface energy elevating structural features such as twinning might be advantageously exploited for the transfer of crystal growth behaviour to result in the formation of economically competitive, catalytically active core-shell structures. Notably, chronoamperometry (CA) experiments at 0.84 V also indicated that the electrochemical stability of both Pt hierarchical structures toward MOR is superior to those of nanorods (see Fig. S3 in the ESI). In accordance with this observation, no discernible difference was observed between the surfactant removed Pt₃Ni@Pt hierarchical nanostructure and the Pt₃Ni@Pt nanostructure after electrochemical measurements (see Fig. S4 in the ESI).

There have been numerous attempts to improve the catalytic performance for oxygen reduction reaction (ORR), which is the major cathode reaction in fuel cells, by using structure-engineered Pt and Pt alloy nanoparticles.²⁶ Therefore, we also investigated the electro-catalytic properties of Pt nanostructures for ORR as shown in Fig. 3.

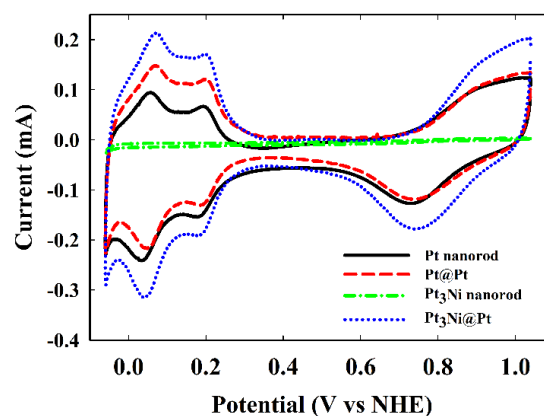


Fig. 3 Cyclic voltammograms of Pt nanostructures-modified GCE in O₂-saturated 0.5 M H₂SO₄ electrolyte solution. Scan rate was 100 mV/s.

A similar catalytic activity trend for MOR was also observed for ORR. Pt₃Ni@Pt shows significantly enhanced (nearly 100% increase) current density over Pt nanorod, while Pt@Pt exhibits relatively small enhancement of catalytic property. It is quite intriguing to note similar activity enhancement reported for other core-shell nanoparticles with core-shell lattice

mismatch^{10-13,21,22,24} and therefore the design concept of core-shell and thorough understanding of the nature of core-shell mismatch might require further investigation for the development of better performing ORR catalysts. The remaining challenge for our work is to prepare hierarchical core-shell structures with facet-controlled high index Pt facets, preferably with twinning boundaries exposed. It has been demonstrated that high index Pt facets are particularly useful for electrocatalytic applications.^{1,27,28} In the case of Pt₃Ni nanoparticles, {111}Pt₃Ni is most active among low index Pt₃Ni crystal surfaces. Therefore, it is intriguing to prepare a hierarchical nanostructure with a core-shell mismatch as well as exposed {111}Pt₃Ni facets.

Conclusions

In summary, we have successfully demonstrated a proof-of-concept to introduce highly energetic structural features, namely elongated twinning boundary coastline and lattice mismatch, in the hierarchically dendritic nanostructures for enhanced electrocatalytic performances in fuel cell electrode applications. With the usage of axially twinned nanorods, the twinning properties of the nanorod surface could be epitaxially transferred to the newly grown crystallites. The highly energetic nature of twinning boundary in the substrate nanorod seems to provide excellent epitaxial growth sites because the growth of new crystallites is favourable for the thermodynamically desired surface energy stabilization process. We believe that the usage of other twinned core structures would lead to a group of highly active hierarchically dendritic nanocatalysts. In addition, facet control of the hierarchical nanostructures might lead to further catalytic performance improvement, and we are currently investigating this possibility also.

Acknowledgements

This work was supported by NRF-2013R1A2A2A 01015168, NRF 2010-0020209, NRF 2014M3A6B2, NRF-2012R1A1A 1040285. We thank KBSI for allowing the usage of their HRTEM instruments.

Notes and references

^a Department of Chemistry and Research Institute for Natural Sciences, Korea University, Seoul 136-701 (Korea). Tel: +82 2 3290-3139; E-mail: kylee1@korea.ac.kr.

^b Korea Basic Science Institute (KBSI), Seoul 136-713 (Korea).

^c Department of Chemistry, Konkuk University, Seoul, 143-701 (Korea). Tel: +82 2 450 3629; E-mail: sjkwon@konkuk.ac.kr.

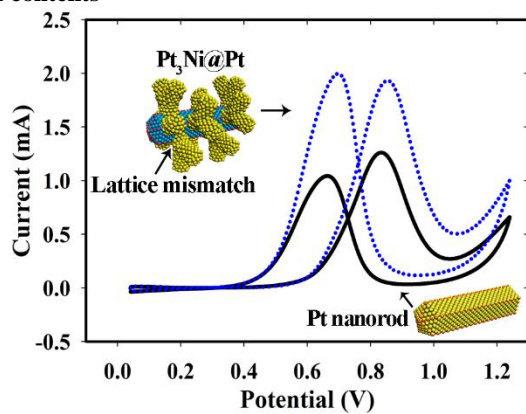
^d Department of Chemical and Biological Engineering, Korea University, Seoul 136-701 (Korea).

† Electronic Supplementary Information (ESI) available: [Experimental section, Figure S1 to S5]. See DOI: 10.1039/b000000x/

1 N. Tian, Z. Zhou, S. Sun, Y. Ding and Z. L. Wang, *Science*, 2007, **316**, 732.

- 2 X. Huang, S. Tang, H. Zhang, Z. Zhou and N. Zheng, *J. Am. Chem. Soc.*, 2009, **131**, 13916.
- 3 Z. Lin, H. Chu, Y. Shen, L. Wei, H. Liu and Y. Li, *Chem. Commun.*, 2009, **45**, 7167.
- 4 K. Lee, M. Kim and H. Kim, *J. Mater. Chem.*, 2010, **20**, 3791.
- 5 C. L. Lu, K. S. Prasad, H. L. Wu, J. A. A. Ho and M. H. Huang, *J. Am. Chem. Soc.*, 2010, **132**, 14546.
- 6 F. Wang, C. Li, L. D. Sun, H. Wu, T. Ming, J. Wang, J. C. Yu and C. H. Yan, *J. Am. Chem. Soc.*, 2011, **133**, 1106.
- 7 X. Huang, Z. Zhao, J. Fan, Y. Tan and N. Zheng, *J. Am. Chem. Soc.*, 2011, **133**, 4718.
- 8 C. W. Yang, K. Chanda, P. H. Lin, Y. N. Wang, C. W. Liao and M. H. Huang, *J. Am. Chem. Soc.*, 2011, **133**, 19993.
- 9 B. Lim, M. Jiang, P. H. C. Camargo, E. C. Cho, J. Tao, X. Lu, Y. Zhu and Y. Xia, *Science*, 2009, **324**, 1302.
- 10 S. E. Habas, H. Lee, V. Radmilovic, G. A. Somorjai and P. Yang, *Nat. Mater.*, 2007, **6**, 692.
- 11 S. Alayoglu, A. U. Nilekar, M. Mavrikakis and B. Elchhorn, *Nat. Mater.*, 2008, **7**, 333.
- 12 P. Strasser, S. Koh, T. Anniyev, J. Greeley, K. More, C. Yu, Z. Liu, S. Kaya, D. Nordlund, H. Ogasawara, M. F. Toney and A. Nilsson, *Nat. Chem.*, 2010, **2**, 454.
- 13 D. Wang, H. L. Xin, R. Hovden, H. Wang, Y. Yu, D. A. Muller, F. J. DiSalvo and H. D. Abruna, *Nat. Mater.*, 2013, **12**, 81.
- 14 N. T. Khi, J. Yoon, H. Kim, S. Lee, B. Kim, H. Baik, S. J. Kwon, K. Lee, *Nanoscale*, 2013, **5**, 5738.
- 15 J. Yoon, N. T. Khi, H. Kim, B. Kim, H. Baik, S. Back, S. Lee, S.-W. Lee, S. J. Kwon, K. Lee, *Chem. Commun.*, 2013, **49**, 573.
- 16 L. Ruan, E. Zhu, Y. Chen, Z. Lin, X. Huang, X. Duan and Y. Huang, *Angew. Chem. Int. Ed.*, 2013, **52**, 12577.
- 17 C. H. Kuo and M. H. Huang, *Langmuir*, 2005, **21**, 2012.
- 18 J. L. Elechiguerra, J. Reyes-Gasga, M. J. Yacaman, *J. Mater. Chem.*, 2006, **16**, 3906.
- 19 Y. Yu, Q. Zhang, J. Xie, X. Lu, J. Y. Lee, *Nanoscale*, 2011, **3**, 1497.
- 20 R. Imbeault, A. Pereira, S. Garbarino and D. Guay, *J. Electrochem. Soc.*, 2010, **157**, B1051.
- 21 E. P. Lee, Z. Peng, W. Chen, S. Chen, H. Yang and Y. Xia, *ACS Nano*, 2008, **2**, 2167.
- 22 G. Chen, Y. Tan, B. Wu, G. Fu and N. Zheng, *Chem. Commun.*, 2012, **48**, 2758.
- 23 J. Zhang, H. Yang, J. Fang and S. Zou, *Nano Lett.*, 2010, **10**, 638.
- 24 V. R. Stamenkovic, B. Fowler, B. S. Mun, G. Wang, P. N. Ross, C. A. Lucas and N. M. Markovic, *Science*, 2007, **315**, 493.
- 25 H. Kim, N. T. Khi, J. Yoon, H. Yang, Y. Chae, H. Baik, H. Lee, J.-H. Sohn, K. Lee, *Chem. Commun.*, 2013, **49**, 2225.
- 26 M. K. Debe, *Nature*, 2012, **486**, 43.
- 27 T. Yu, D. Y. Kim, H. Zhang and Y. Xia, *Angew. Chem. Int. Ed.*, 2011, **50**, 2773.
- 28 B. Yu, H. B. Wu, X. Wang and X. W. Lou, *Angew. Chem. Int. Ed.*, 2013, **52**, 12337.

Table of contents



Introduction of twinning boundary elongation and lattice mismatch to the hierarchical and dendritic Pt₃Ni@Pt nanostructure by heteroepitaxial twinning transfer from five-fold twinned Pt₃Ni nanorod leads to a great enhancement in the electrocatalytic performance in MOR and ORR.